Review

Check for updates

Characterizing the wetting behavior of 2D materials: a review

Chuanli Yu, Zhaohe Dai[*] iD

Department of Mechanics and Engineering Science, State Key Laboratory for Turbulence and Complex Systems, College of Engineering, Peking University, Beijing 100871, China.

[*]**Correspondence to:** Prof. Zhaohe Dai, Department of Mechanics and Engineering Science, State Key Laboratory for Turbulence and Complex Systems, College of Engineering, Peking University, Beijing 100871, China. E-mail: daizh@pku.edu.cn

Abstract

A comprehensive understanding of the interaction between liquids and two-dimensional (2D) materials is pivotal for the manipulation, transfer, and assembly of 2D materials across a wide range of applications, from liquid cell microscopy to hydrovoltaics. This review discusses this interaction by surveying the intrinsic wettability of suspended 2D materials and the apparent wettability of substrate-supported 2D materials, both of which have recently been revealed through water contact angle (WCA) experiments. We discuss important factors that can affect the apparent WCA, including thin film elasticity, surface contamination, and the microstructure and electronic state of the underneath substrate. We also discuss some microscopic-level insights into the 2D material-liquid interface that have recently been provided via spectroscopy characterizations and surface energy measurements. By discussing the latest experimental advancements in characterizing the interaction between 2D materials and liquid droplets, this review aims to inspire future theoretical progress capable of unraveling the intricate and occasionally contradictory wetting behavior observed in 2D material systems.

Keywords: 2D materials, wettability, water contact angle, elastocapillarity, surface energy

INTRODUCTION

Graphene and a variety of other two-dimensional (2D) materials have attracted considerable attention due

to their exceptional physical properties, which hold tremendous potential across a wide range of applications, including electronics, optoelectronics, nanocomposites, sensors, and more[1-6]. Beyond their unique properties, the atomically thin structure of 2D materials is perhaps their most prominent feature, resulting in ultra-large volume-to-surface ratios that underscore the paramount importance of understanding 2D material surfaces and interfaces[7,8]. Notably, the wetting property of 2D materials, which characterizes the affinity of the solid surface to liquid, has been the subject of extensive investigation over the past decade[9-16]. This investigation is motivated not only by its fundamental importance but also by its potential implications for various applications such as ionic sieves[17-20], coating technology[21,22], photovoltaic devices[23,24], water permeation[25], energy storage[26], and hydrovoltaics[27]. However, the combination of surface forces, the slenderness, and the atomic thin nature of 2D materials has given rise to a plethora of intricate wetting phenomena[28,29], leading to occasionally contradictory observations and necessitating further studies[15,30-33].

Here, we present an overview of recent experimental progress concerning the wetting behavior of 2D materials at both macroscopic and microscopic levels (refer to the schematic illustration in Figure 1). The macroscopic perspective focuses on water contact angles (WCAs) measured directly through sessile droplets on supported and suspended 2D materials [Figure 1A and B]. Additionally, we discuss various factors, such as surface mechanics and chemistry, that influence the observed WCA. The microscopic perspective focuses on the WCA inferred indirectly through the examination of interfacial water structures and the measurement of surface energies [Figure 1C and D]. This review does not aim to comprehensively cover all aspects of wetting phenomena in 2D materials. Instead, it aims to highlight the multiscale nature of this emerging class of wetting problems and to stimulate future theoretical advancements capable of unraveling the intricate and occasionally contradictory wetting behavior observed in 2D material systems. We encourage readers to explore relevant reviews and perspectives from different angles, including surface chemistry/physics of graphene[7,34], mechanics of 2D material interfaces[8], interaction of 2D materials with liquids[35], interfacial water structure on graphene[13], and wettability of graphene[29,36].

WETTING PHENOMENA IN 2D MATERIALS

Before discussing experimental progress on characterizing liquid droplet-2D material interactions, we first discuss several intriguing wetting phenomena, specifically those that have found some uses. One notable example is the observation of condensation figures, which manifest as arrays of droplets that emerge when vapor condenses onto a substrate coated with graphene. These condensation figures offer a visual representation of the lateral geometry of graphene that is otherwise imperceptible to the naked eye [Figure 2A][37]. Furthermore, the shape of the droplet has been identified as a means to determine the crystal orientation of anisotropic 2D materials, such as black phosphorus (BP) [Figure 2B and C][38]. Besides, it could potentially serve as an indicator of the principle orientation of the stress state within a stretched film as well[39]. However, for a more quantitative understanding of the droplet geometry, it is crucial to elucidate the role played by the substrate in determining the wetting conditions at the triple line, which we will discuss shortly.

Another intriguing class of wetting phenomena in 2D materials arises when the liquid is confined at the interface between the 2D material and the substrate[40]. In such instances, both elastic and capillary forces come into play, differentiating them from the classical wetting problem involving droplets on a rigid substrate[41-43]. While not entirely understood, the combination of such forces has been somehow useful for the clean and nondestructive transfer of 2D materials[44-48]. Moreover, it has facilitated the manipulation of 2D materials, including bending, folding, and rolling[8,49]. Importantly, the unique interaction between the liquid and solid phases has been found to impact the static and dynamic behavior of the system, although
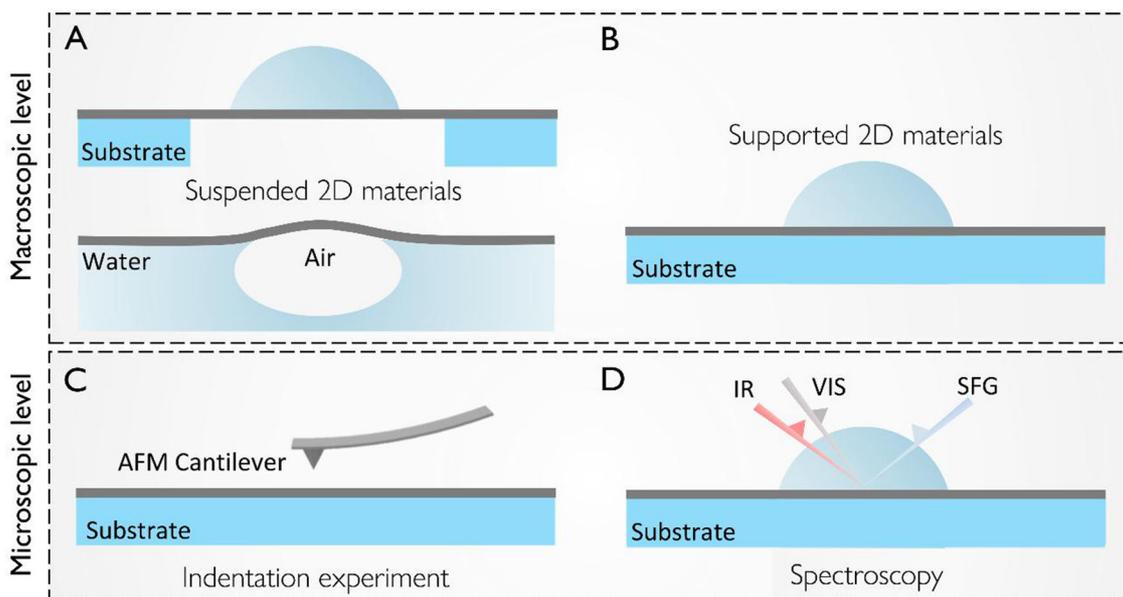
Figure 1. Schematic illustration of various experimental methods to characterize the wetting behavior of 2D materials. Macroscopic level methods include WCA measurement on (A) suspended and (B) supported 2D materials, while microscopic level methods include the wettability indirectly implied by (C) surface energy measurements and (D) spectroscopy characterizations. AFM: Atomic force microscope; IR: infrared pulse; VIS: visible pulse; WCA: water contact angles; 2D: two-dimensional.
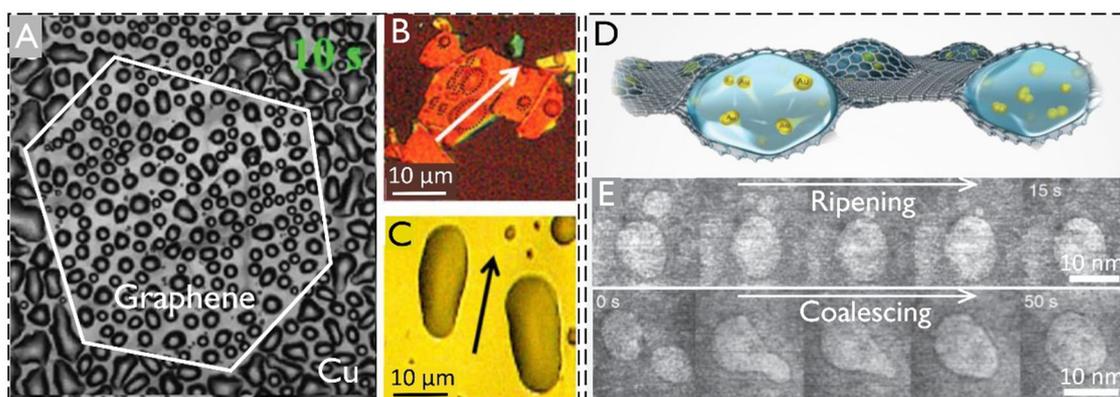
Figure 2. (A) Water-vapor assisted visualization of monolayer graphene[37]; Anisotropic liquefaction process of water droplets on the surface of (B) few-layer and (C) thick BP[38]; (D) Schematic illustration of GLCs that has been useful in liquid-phase electron microscopy technique[59]; (E) *In situ* TEM images of two different merging modes of adjacent nanobubbles observed in GLCs[63]. Figures are adapted from references[37,38,59,63] with permission. BP: Black phosphorus; GLCs: graphene liquid cells; TEM: transmission electron microscope.

the underlying mechanisms require further investigation. For example, the liquid-solid interaction has been reported to significantly reduce the in-plane stiffness of graphene, which is crucial information for the development of emerging techniques based on 2D material microfluidic devices[50,51]. On the other hand, it has been found that the elasticity of 2D materials covering a thin liquid layer can prevent the dewetting of the confined liquid layer[52]. In cases where dewetting does occur, the presence of 2D materials has led to various dewetting patterns, contingent upon the flexibility of the covering 2D material layer[42,53,54]. Currently, the precise conditions, mechanisms, and rate of this dewetting phenomenon remain unclear [particularly the role played by the van der Waals (vdW) interactions[55]], but one may expect that

unraveling these aspects could help to develop novel transfer methods for making 2D material devices with large and clean interfaces[45].

The confinement of liquid at the flexible 2D material-2D material interface also presents a unique wetting phenomenon[56]. This flexible confinement has given rise to GLCs [Figure 2D], which have become a powerful platform for liquid-phase electron microscopy techniques, facilitating the visualization of nanostructures of wet samples or nanomaterials in liquids[57-59]. For example, Yuk *et al.* successfully encapsulated platinum salt precursors within GLCs, enabling real-time electron microscopy imaging of the nucleation and growth of platinum nanoparticles with exceptional spatial resolution[60]. Similarly, this imaging technique has been applied to other liquid-containing samples, such as synthetic polymers, lipid assemblies, and DNA-enzyme complexes[61]. In addition, nanobubbles in GLCs have been employed to investigate gas transport mechanisms at the nanoscale [Figure 2E][62,63], for which two distinct growth dynamics (i.e., ripening and coalescing) have been observed[62,63]. The merging of nano-droplets in GLCs has also been reported. However, molecular dynamics simulations suggested a ripening mechanism[64] for such merging, while recent experiments revealed a coalescing mechanism induced by the loss of symmetry in the elastic deformation of graphene sheets[65]. Furthermore, in situations where the number of confined water molecules is limited, these molecules can be compelled to adopt an ice-like structure, challenging the continuum description of liquid behavior[66,67]. Consequently, further investigations are imperative to understand the transition between the continuum and discrete regimes and the dynamics involved in their merging. Such understanding may yield new insights into the self-cleaning or self-aggregation of interfacial contaminants at 2D material interfaces, which is particularly useful for device applications[68].

WETTABILITY OF SUSPENDED GRAPHENE

Although achieving a comprehensive understanding of the wetting phenomena in 2D materials discussed above requires a combination of dynamical modeling and experiments, it is crucial to begin by characterizing the static wettability of these materials, specifically their WCAs. However, until recently, this seemingly straightforward experiment had only been conducted on suspended graphene with the fabrication of large, clean graphene and the utilization of micro-droplet condensation in an environmental scanning electron microscope (ESEM)[15]. The earlier studies primarily focused on substrate-supported graphene. However, supported systems have introduced vulnerabilities due to the influence of the underlying substrate, contamination in ambient conditions, and other factors, leading to a misconception that graphene is hydrophobic[30,69]. Thus, in this section, our focus lies on the experimental advancements in measuring the WCA of suspended graphene, which may offer insights into the intrinsic wettability of graphene[15,70,71].

Prydatko *et al.* were the first to measure the WCA of suspended graphene[70]. The particular method (captive bubble method) they used is to introduce a gas bubble under a chemical vapor deposition (CVD) grown monolayer graphene that is positioned at the water-air interface, as depicted in Figure 3A(i)[70]. A key technical challenge in such experiments is the limited survival time of the bubble underneath the graphene, typically lasting only a few seconds to a few minutes, as the surface tension of water can readily damage graphene. To determine the contact angle, Neumann's triangle relation was utilized, as shown in Figure 3A (ii)[70]. However, it remains unclear how the elastic forces in the deformed graphene might influence this triangle relation and the resulting WCA[72]. Despite this uncertainty, the experimental results, obtained by disregarding the effects of elasticity, indicated that the contact angles of graphene ranged between 37° and 44°, confirming the intrinsic hydrophilicity of graphene. Notably, these contact angles were noticeably influenced by the humidity of the surrounding air [Figure 3A(iii)][70]. This observation suggests that the line forces acting on the triple line not only interact with graphene but also with the vapor physically separated
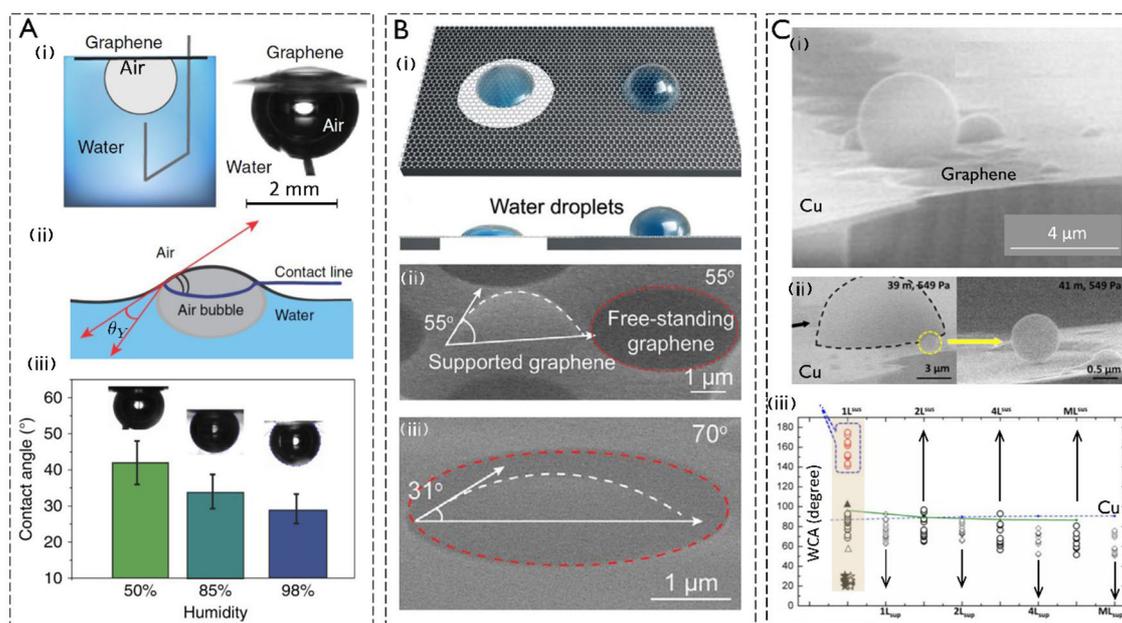
Figure 3. WCA measurements on suspended graphene. (A) (i) Schematic and picture of the captive bubble method for measuring the WCA on suspended graphene; (ii) Surface energy balance at the triple line indicated by the Neumann's triangle; (iii) Measured WCA as a function of relative humidity of air[70]; (B) (i) Schematic of micro-droplets on graphene that is supported by a hole-patterned substrate; (ii) ESEM image of a water droplet on graphene that is supported by an Au/carbon substrate with a 70° tilt angle of sample stage with respect to the electron beam; (iii) ESEM image of a water droplet on clamped, suspended graphene with a 70° tilt angle[15]; (C) (i) ESEM image of droplets condensed on monolayer graphene sitting on a trench; (ii) ESEM image of droplets with and without contact with the substrate-supported region; (iii) WCA statistics on supported and suspended monolayer and multilayer graphene[71]. Figures are adapted from references[15,70,71] with permission. ESEM: Environmental scanning electron microscope; WCA: water contact angle.

by graphene. In other words, graphene exhibits wetting translucency or partial "wetting transparency", a term to be extensively discussed in substrate-supported systems[28,33].

Zhang *et al.* utilized a unique approach reminiscent of the classical WCA measurement, albeit with markedly smaller droplets (measuring in microns and sub-microns in radii, as depicted in Figure 3B)[15]. The authors utilized ultraclean graphene obtained by using Cu foam to suppress the formation of amorphous carbon on the graphene surface during the CVD growth[73]. To avoid any polymer residues, the as-grown graphene was transferred to a hole array using a non-polymer transfer method for WCA measurement[59]. Microdroplets on graphene are condensed by increasing the chamber water pressure from a vacuum, followed by direct ESEM observation. Figure 3B(ii) and (iii) illustrates the contact angles observed for micro-droplets condensed on substrate-supported and suspended graphene, which are approximately 55° and 31°, respectively[15]. These results further confirm the intrinsic hydrophilicity and wetting translucency of graphene. Notably, the presence of airborne hydrocarbon, amorphous carbon, and polymer residues on suspended graphene was found to increase the apparent contact angle to around 50°, 60°, and 70°, respectively. However, Wang *et al.* reported a contradictory result - a contact angle close to 180° for monolayer graphene suspended on a trench[71]. In this case, the micro-droplet nucleation is achieved by adjusting the vapor pressure in the chamber, and the pressure rate is controlled to allow the steady-state growth of the condensate [Figure 3C(i)][71]. The authors claimed that this non-wetting behavior occurred only when both sides of the suspended monolayer graphene were exposed to the environment, despite such experimental conditions being identical to those used in the study by Zhang *et al.*[15]. However, despite this contradiction, the abnormal non-wetting phenomenon appears to be robust, as demonstrated in

Figure 3C(ii): when the droplet grows and reaches the supported graphene, it suddenly spreads to form an approximately hemispherical shape, while the newly condensed nano-droplet on the suspended graphene retains a perfect spherical shape. Figure 3C(iii) shows WCAs observed on graphene with different numbers of layers, where this non-wetting phenomenon was not observed in bilayer and multilayer graphene systems, whether supported or suspended[71]. These dramatically different WCAs in Figure 3B and C, along with the slight dependence on droplet size, might warrant further investigation[15,71].

WETTABILITY OF SUPPORTED 2D MATERIALS

In contrast to the limited number of reports on the wettability of suspended 2D materials, there is a significant body of experimental literature dedicated to substrate-supported 2D materials[9,11,12,31-33,74-76]. Within this context, a particularly intriguing question that has garnered attention is whether the effective vdW interaction between liquid and 2D materials is influenced by the underlying substrate.

Rafiee *et al*. compared the static WCA measured on bare and graphene-coated substrates[31]. They found that the presence of graphene between the water droplet and the bare substrate does not significantly affect the apparent contact angle until the layer number of graphene exceeds 4 [Figure 4A][31]. The phenomenon that the interaction between substrate and liquid can completely penetrate single-layer or few-layer 2D materials is called "wetting transparency". To further investigate this phenomenon, the authors employed molecular dynamics simulations to examine the adsorption energy of water on Cu substrates with varying numbers of graphene layers [Figure 4B]. They discovered that the introduction of a monolayer of graphene resulted in minimal changes in the adsorption energy, thus explaining the observed wetting transparency. However, a number of groups have performed similar wetting experiments on supported graphene systems but have arrived at different conclusions. These studies categorized graphene as either wetting transparent[10,31,77], translucent[28,33], or opaque[32,78,79]. For instance, Shih *et al*. demonstrated that the coating of graphene can render hydrophobic substrates more hydrophilic and hydrophilic substrates more hydrophobic, indicating partial wetting transparency or wetting translucency of graphene[28]. In contrast, Raj *et al*. emphasized the limitations of static contact angles and proposed the use of advancing contact angles to better understand graphene's wettability[32]. Their results indicated that the advancing contact angle is almost independent of the number of graphene layers, suggesting the wetting opacity of graphene.

In Figure 4C, we present the WCAs of clean suspended graphene[15] and aged graphite[80] as the two extreme cases. Additionally, a dashed line is included to represent complete wetting transparency, indicating that the apparent WCA of the supported graphene (θ_{App}) is identical to that of the underlying substrate ($\theta_{Substrate}$). It is clear that the majority of experimental data fall between these two limiting cases, with only a few data points approaching the dashed line representing complete wetting transparency. Although these studies have not yet reached a consistent conclusion regarding the wetting transparency of graphene, the considerable scattering observed in θ_{App} measured on various substrates suggests that the substrate may have some influence on the WCA of the graphene it supports. Additional evidence supporting the existence of substrate effects can be found in experiments that measured WCAs on partially suspended graphene[16]. It is demonstrated that the hole area of the substrate can regulate the WCAs observed on the graphene surface. Furthermore, Ondarçuhu *et al*. achieved the control of the area fraction of suspended graphene from 0% to 95% using nanotextured substrates[14]. They concluded that approximately 80% of the long-distance water-substrate interaction could be screened by a monolayer of graphene, providing further support for the influence of the substrate on wetting behavior.

The extent to which a 2D material screens the long-range liquid-substrate interaction or exhibits wetting transparency is influenced by multiple factors. For example, Figure 4C presents compelling evidence
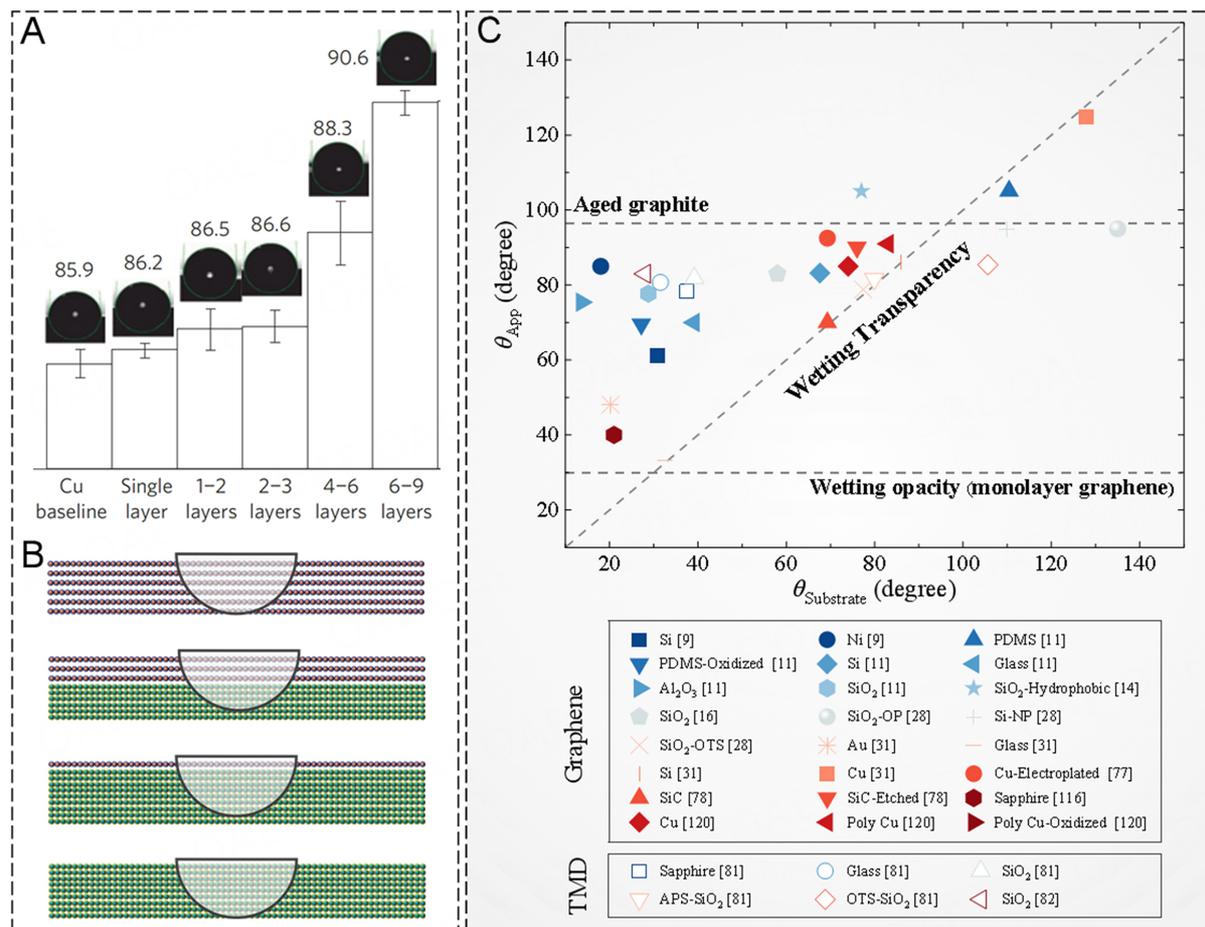
Figure 4. Wetting transparency of atomically thin 2D materials in Figure 4A-C. (A) WCA on Cu and Cu-supported graphene of different numbers of layers[31];(B) Schematic of the interaction range of water molecules on the bare substrate and substrate-supported graphene; (C) Summary of experimentally measured WCAs on the bare substrate $\theta_{Substrate}$ and on substrate-supported monolayer 2D materials θ_{App}[9,11,14,16,28,31,77,78,81,82,116,120]. The horizontal dashed lines represent the contact angles of aged graphite (around 97°) and clean, suspended monolayer graphene (around 30°), respectively, while the oblique dashed lines represent the condition for wetting transparency of 2D materials, i.e., $\theta_{Substrate} = \theta_{App}$. Figures A is adapted from reference[31] with permission. WCA: Water contact angle; 2D: two-dimensional.

highlighting the significance of 2D material thickness. WCAs measured on monolayer transition metal dichalcogenides (TMDs), which are considerably thicker than graphene, demonstrate independence from the substrate[81,82]. This observation strongly suggests the wetting opacity of TMDs or their effective screening of the liquid-substrate interaction[82-85]. Simulations based on density functional theory (DFT) indicate that the specific screening effect relies on the band gap and dielectric constant of the material, showing relatively weaker effects for semiconducting and insulating 2D materials[86]. Molecular dynamics Simulations have demonstrated that the interaction between the substrate and the droplet can partially penetrate the single-layer insulating hexagonal boron nitride (hBN)[87] and also depends on the nature of hBN edges (zigzag or armchair) when a nanostructured hBN substrate is used[88]. However, experiments conducted on hBN have demonstrated wetting opacity, wherein hBN completely screens the drop-substrate interaction[89]. In addition, recent experiments have revealed that the polarities of liquids and substrates also impact the detailed screening effect or wetting transparency of 2D materials[11]. Nonetheless, precisely understanding the screening effect of 2D materials through WCA experiments on supported systems can be challenging due to various uncontrollable factors that can influence the apparent WCAs. In the following discussion, we will briefly address these factors.
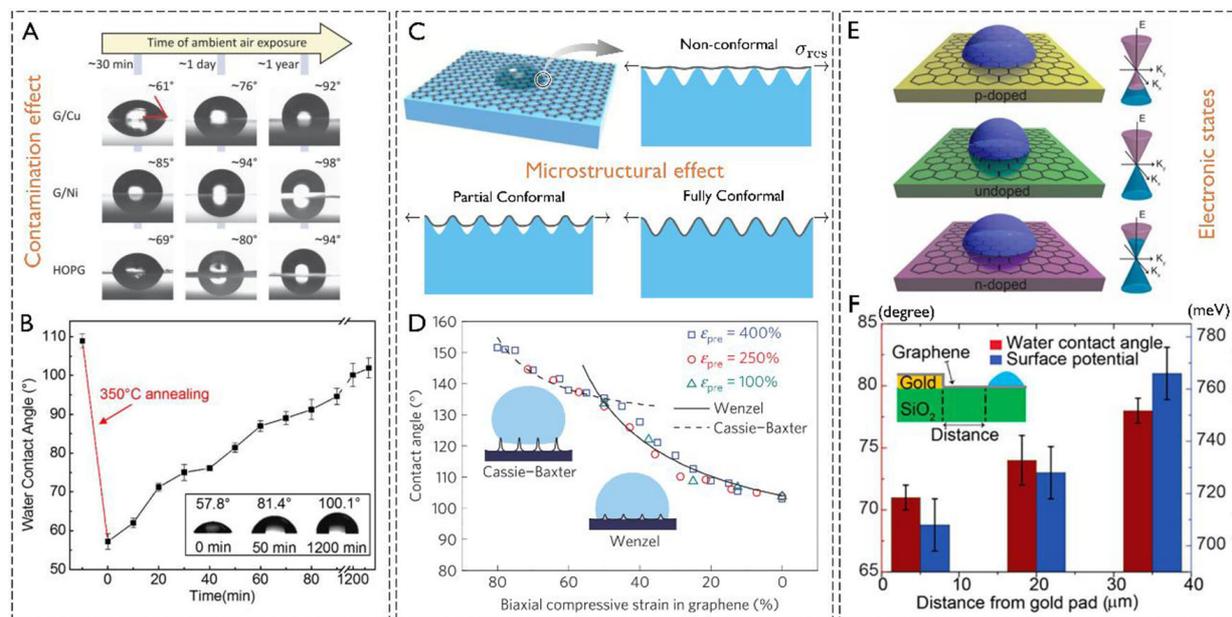
Figure 5. Factors that can impact the apparent contact angle measured on the supported 2D material systems. (A) WCAs as a function of exposure time for HOPG and graphene on Cu and Ni substrates[9]; (B) WCA of a 20-nm-thick InSe on SiO$_2$ before and after 350 °C thermal annealing[90]; (C) Schematic of three possible contact modes between a 2D material and a substrate, including non-conformal, partially conformal, and fully conformal; (D) WCA on polydimethylsiloxane-supported graphene as a function of biaxial compressive strain applied to the substrate[104]; (E) Schematic illustration of the graphene wettability being modulated by doping induced Fermi level shifts[105]; (F) WCA and surface potential of graphene as functions of the distance from the gold pad in a metal - graphene heterojunction[105]. Figures are adapted from references[9,90,104,105] with permission. HOPG: Highly oriented pyrolytic graphite; WCA: water contact angle; 2D: two-dimensional.

FACTORS INFLUENCING THE APPARENT CONTACT ANGLE

The surface chemistry of 2D materials has been observed to change when exposed to air, which is considered one of the major reasons for the inconsistent apparent contact angles reported[76]. Specifically, airborne contaminants present in the air can spontaneously adhere to the surface of 2D materials, resulting in reduced hydrophilicity[9,76]. For example, Figure 5A illustrates the WCAs measured on Ni- and Cu-supported graphene and the WCA of highly oriented pyrolytic graphite (HOPG) over time in air[9]. It is evident that the WCAs of all samples increase rapidly within the initial 30 min of exposure and gradually stabilize to become hydrophobic (> 90°). This transition from hydrophilic to hydrophobic behavior (i.e., aging) has been observed in various 2D material systems, including TMDs[82-85]. Recent experiments on InSe films have also shown that the aging behavior is nearly independent of the substrate used to grow these films (such as silicon, glass, nickel, copper, and aluminum oxide)[90]. Furthermore, it has been discovered that thermal annealing of the aged samples in a furnace at 350 °C for 2 h can rejuvenate the WCA of InSe films by removing absorbed contaminants from their surfaces [Figure 5B][90]. It is important to note that ultraviolet (UV) irradiation can also be utilized to eliminate surface contamination on 2D material surfaces[76], but prolonged exposure to UV radiation may introduce defects to their atomic structure[14]. Additionally, it should be noted that surface contamination can be introduced during the transfer process of 2D materials, particularly when polymer stamps are used, and this can affect their apparent contact angle as well[15].

The surface roughness of substrate-supported 2D materials also plays an important role in determining the apparent WCAs, even though 2D materials themselves have been considered atomically smooth[28,32,91]. In

the presence of substrate roughness, previous studies have classified the contact proximity between a 2D material and its substrate into three modes: fully conformal, partially conformal, and non-conformal, as illustrated in Figure 5C[8]. The specific mode might be determined by the interplay between elastic forces and adhesive forces[92,93] and potentially influenced by how careful this contact is made (i.e., the "dewetting" dynamics)[94-96]. However, it remains unclear how different contact modes differentiate the contributions of the substrate effect to the interaction between the liquid and substrate. Furthermore, the role of elastic membrane forces in different contact configurations is of importance in the force balance at the triple line or contact line (and consequently the apparent WCA), but this aspect remains unexplored[97-99]. On the other hand, wrinkles, folds, or crumples in 2D materials can be produced when such elastic forces are compressive[100-102], which have found uses in tuning the surface wettability[103]. For example, Zang *et al.* observed a transition in the wetting state of polymer-supported graphene from the Cassie-Baxter to Wenzel state as the compressive strain on the substrate increased, leading to the graphene becoming more crumpled [Figure 5D][104]. Choi *et al.* further showed the control of the WCA on MoS_2 from 80° to 155° by making use of both initial surface microstructures and mechanical strains[74].

The Fermi level of graphene, which can be directly affected by the underlying substrate, can also modulate its apparent hydrophilicity, as extensively discussed in a notable review by Snapp *et al.*[35]. Here, two specific examples are discussed. Ashraf *et al.* explored the influence of Fermi level modulation on the contact angle of CVD-grown graphene by doping the underlying substrate, as depicted in Figure 5E[105]. They used p-doping and n-doping to achieve a change of approximately 300 meV in the work function and up to a 13° alteration in the contact angle. Furthermore, they manipulated the surface potential of graphene by creating a lateral metal-graphene heterojunction [Figure 5F], resulting in a decrease in the contact angle when the droplet was positioned closer to the graphene-gold junction. Hong *et al.* reported similar observations and proposed, through a combination of experiments and DFT simulations, that the substrate effect on the contact angle of graphene could be attributed not to the vdW interaction between water molecules and the substrate through the partially "transparent" graphene layer but rather to the modification of the Fermi level of graphene by the substrate or dopants (either p-doping or n-doping), and consequently, the interaction of graphene with polar water molecules[106]. Further experiments, in addition to WCA measurements, are needed to clarify this argument.

WETTABILITY SUGGESTED BY SURFACE ENERGY MEASUREMENTS

To elucidate the intriguing and complex wetting behavior observed in 2D material systems, characterizations of vdW interactions among liquids, 2D materials, and substrates are necessary. In this regard, probe-based surface/interface energy measurements provide a powerful tool. On the one hand, the apparent WCA can be predicted theoretically by measuring the 2D material-vapor surface energy (γ_{sv}) and 2D material-liquid surface energy (γ_{sl}) and using the Young's law $\cos\theta_{App} = (\gamma_{sv} - \gamma_{sl})/\gamma$, where γ is the surface tension of the liquid. Besides, the measurement of the 2D material-liquid adhesion energy (W_{ad}) can be employed to calculate the WCA using $W_{ad} = \gamma(1 + \cos\theta_{App})$. On the other hand, examining the force-displacement relation or traction-separation relation in surface energy measurements can provide further quantitative insight into the long-range vdW interactions of 2D materials[8].

For example, van Engers *et al.* performed surface energy measurements of graphene coating two cylindrical epoxy lenses [Figure 6A][107]. They employed a surface force balance apparatus and utilized the JKR theory (the Johnson-Kendall-Roberts theory) to establish a relationship between the measured pull-off force and the surface energy of the supported graphene in different mediums. On the one hand, the measured surface energies for few-layer and single-layer graphene are 119 ± 3 mJ/m² and 115 ± 4 mJ/m², respectively. Both values are significantly higher than that of bare epoxy resin, suggesting the wetting opacity of graphene on
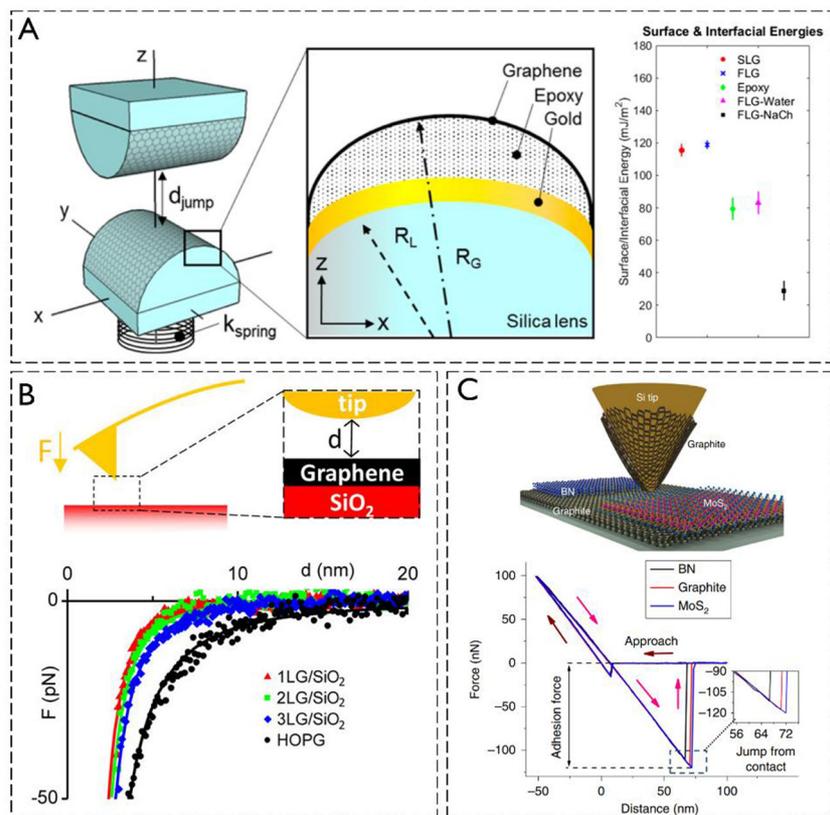
Figure 6. Measurement of surface energy or forces of supported 2D materials. (A) Schematic of the surface force balance apparatus based on graphene-coated epoxy cylinders and summary of the measured surface energy (based on JKR theory)[107]; (B) Schematic of nanoindentation experiments on graphene-coated silicon oxide substrates and the measured force-separation relationships[110]; (C) Schematic illustration of an AFM tip coated with a thin graphite layer that is brought into contact with 2D materials (top panel) and typical force-distance curves measured on BN, MoS_2, and graphite[112]. Figures are adapted from references[107,110,112] with permission. AFM: Atomic force microscope; FLG: few layer graphene; JKR theory: the Johnson-Kendall-Roberts theory; SLG: single layer graphene; 2D: two-dimensional.

epoxy or the screening of the vdW forces of the epoxy substrate by the graphene layers. On the other hand, the interfacial energy between few-layer graphene and water (FLG-Water) is found to be approximately 83 mJ/m², indicating a WCA of around 60° for graphene (based on Young's relation). This finding is consistent with the initial hydrophilicity observed on fresh graphite[15,70]. However, there is still a need for further clarification regarding the validity of the JKR theory used to obtain these values. This concern arises due to the considerable stiffness of both graphene and the epoxy substrate (which could result in a quantitative difference of up to 33% in the measured pull-off forces)[108] and the impact of surface roughness (which could even result in qualitative differences in stiff systems such as adhesion paradox in pull-off forces)[109].

The screening effect of 2D materials has also been observed in similar nanoindentation experiments conducted by Tsoi *et al.* on a silicon oxide substrate coated with graphene [Figure 6B][110]. The authors directly measured the force experienced by an atomic force microscope (AFM) tip as a function of the tip-graphene distance, which ranged from approximately 5 to 10 nm. Instead of relying on the JKR theory, the authors employed the opposite limit model, considering the vdW interaction between rigid bodies to interpret the force-distance relationships observed. By fitting the experimental data to this model (solid lines in Figure 6B), the authors derived the Hamaker constant for the interaction of the tip with graphene and

with the substrate underneath. It was found that when the substrate was coated with monolayer, bilayer, or trilayer graphene, the Hamaker constant for the tip-substrate interaction was negligible. This suggests that graphene layers effectively screen the vdW interaction between the tip and the substrate, leading to wetting opacity (as discussed in the previous content). However, in a separate study by Suk *et al.*, the adhesive interactions of diamond indenters with bare silicon oxide and graphene-coated silicon oxide showed a clear dependence on the number of graphene layers (i.e., wetting translucency)[111]. A possible explanation for the discrepancy between the findings by Tsoi *et al.*[110] and Suk *et al.*[111] could be that the latter considered the separation between graphene and silicon oxide (which can change the effective distance between graphene and the nanoindenter). In addition, further work is required to clarify the effect of surface roughness in these micro-probe-based measurements[8,93]. For example, it has been demonstrated that the nanoindenter or the probe tip can be coated with graphite to reduce the roughness effect when measuring the vdW interactions between 2D materials [Figure 6C][112].

MICROSCOPIC WETTABILITY INVESTIGATED BY OTHER METHODS

Recently, there has been increasing interest in understanding the wetting behavior of 2D materials by investigating the molecular-level interactions between liquids and solids using spectroscopy techniques. Notably, the microscopic wettability, as revealed by spectroscopic techniques, is not necessarily synonymous with true wettability but may provide additional insights that cannot be obtained solely from macroscopic WCA measurements. One such technique is sum-frequency generation (SFG), which serves as a surface-selective tool for revealing the hydrogen bonding structure of water molecules at the interface[113,114]. Specifically, vibrational and frequency generation (VSFG) spectroscopy of water hydroxyl (OH)-stretch modes at the water-2D material interface can provide direct information on the hydrogen bond distribution of interfacial water molecules[13,114,115]. For example, Kim *et al.* investigated the VSFG spectra of water at the CaF_2/graphene-water interface [Figure 7A][13]. They found that when the number of graphene layers exceeds three, a distinct peak emerged at approximately 3,600 cm^{-1}, representing the VSFG spectral feature of water molecules on hydrophobic surfaces. This peak is generally attributed to OH groups that do not form strong hydrogen bonds with neighboring water oxygen atoms[13]. This finding, therefore, suggested that the water-graphene interface experienced an increase in the number of water molecules with dangling OH groups oriented towards multilayer graphene [Figure 7B][12]. Such significant microstructural transformation in interfacial water as the number of graphene layers increases is impossibly discovered through conventional WCA measurements. The authors also introduced the concept of VSFG wettability, which quantifies the ratio of the area under the strong hydrogen-bonded OH peak to the sum of the areas under the non-hydrogen-bonded (dangling) OH peak and the weak hydrogen-bonded OH peak. Notably, this measure correlated well with the adhesion energy calculated by incorporating the macroscopic WCA into Young's equation [Figure 7C][13].

Similarly, Singla *et al.* employed SFG spectroscopy to investigate the water structure in the vicinity of graphene on a sapphire substrate and explore the influence of graphene on ice nucleation properties[116]. They observed highly ordered water molecules adjacent to graphene, as evidenced by a pronounced SFG peak. In contrast, the bare sapphire surface did not exhibit comparable ordering, implying that the presence of graphene, behaving as hydrophobic or negatively charged, enhances the ordering of water molecules. Interestingly, although liquid water in proximity to graphene demonstrates a degree of order, the ice formed on graphene lacks proton order. In addition, Dreier *et al.* reported that the SFG signal of water molecules at the monolayer graphene interface is predominantly influenced by the substrate; that is, it shows the characteristics of wetting transparency. However, water molecules can occupy the space between the more hydrophilic substrate and the graphene, making the interface more complex[13,117]. Gaire *et al.* recently demonstrated through the VSFG technique that monolayer graphene can screen both vdW and polar (acid-base) interactions[75].
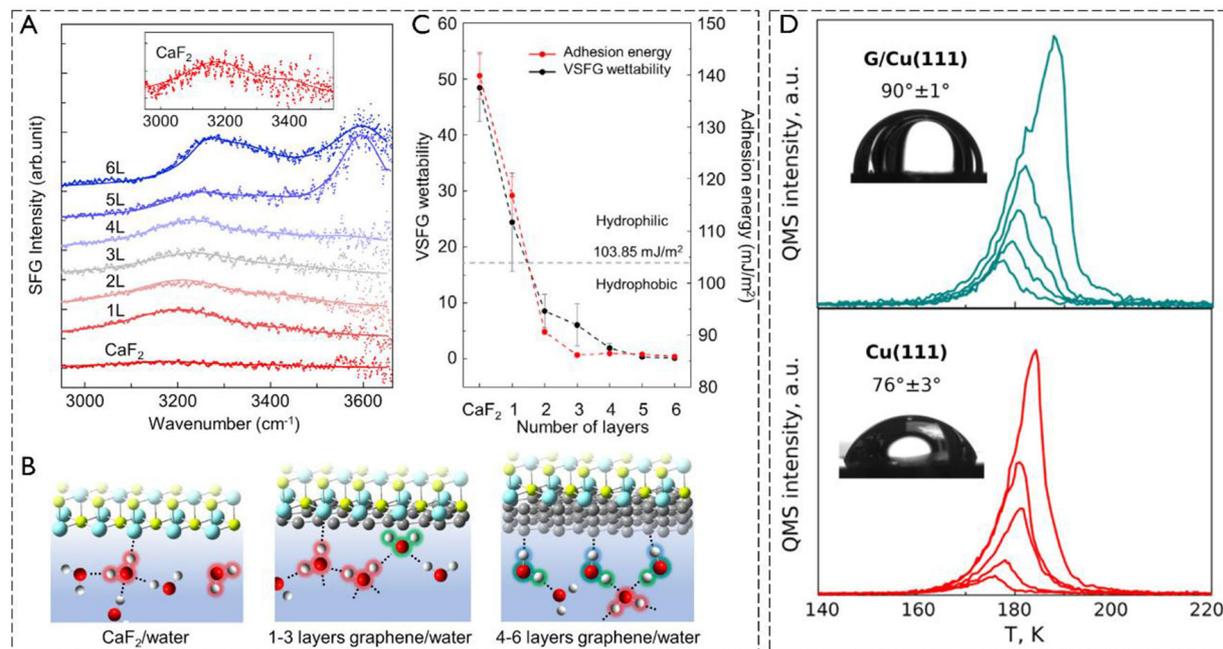
Figure 7. (A) Vibrational sum-frequency-generation spectra of water molecules at the water-graphene interfaces[12]; (B) Schematic diagrams of interfacial water structures on CaF₂ substrate and on CaF₂-supported graphene with varying layer numbers[12]; (C) Correlation between wettability implied by VSFG spectra and water-graphene adhesion energy based on WCA[13]; (D) Thermal desorption spectroscopy curves of graphene grown on Cu (top panel) and bare Cu (bottom panel) at sub-monolayer coverages; Insets in the figures represent the corresponding macroscopically measured WCA[120]. Figures are adapted from references[12,13,120] with permission. VSFG: Vibrational and frequency generation; WCA: water contact angles.

Thermal desorption spectroscopy (TDS), also known as temperature-programmed desorption (TPD), is another technique that enables the investigation of wettability at the molecular level[118,119]. In TPD experiments, water is introduced into a low-temperature ultra-high vacuum (UHV) chamber, and the number of desorbed water molecules is recorded as the temperature is increased, generating a desorption curve provides valuable insights into the thermodynamic and kinetic properties of the water-surface interaction. For example, Figure 7D shows the different kinetic features of water droplets on graphene-coated copper (111) and bare copper (111)[120]. This is specifically manifested as a shared leading edge and a shift to higher temperatures, indicating zero-order desorption in the case of graphene on copper and a mixture of zero-order and first-order desorption characteristics in the case of bare copper, respectively. The observed zero-order dynamics on graphene can be attributed to the 2D equilibrium between individual water molecules and clustered condensed water. This suggests a tendency for water to form multilayer clusters rather than continuous monolayers on graphene. On the other hand, the fractional order kinetics observed on bare copper (111) imply stronger adsorption of water molecules compared to graphene-coated copper (111). Moreover, the slightly more hydrophobic wetting behavior of graphene on copper (111) aligns with the lower affinity between graphene and water observed through contact angle measurements during TPD experiments [Figure 7D][120].

CONCLUSIONS

This review has discussed the wetting properties of 2D materials revealed by both macroscopic and microscopic level characterizations. The focus at the macroscopic level has been the measurement of WCAs on suspended and supported 2D material systems. Emphasis has been placed on the significant variations in observed contact angles within and between these systems, which can be attributed to various factors, such

as the elastic deformation of 2D materials, the presence of contaminants, screening effect, substrate microstructure, and electronic states, among others. The review has also briefly discussed methods that can offer molecular-level insights into the interaction between the substrate, 2D materials, and the liquid, including surface energy measurements and spectroscopy techniques. Looking ahead, it is anticipated that future work may combine WCA measurements with molecular-level experiments, employing both static and dynamic approaches, to unravel the intrinsic wetting behavior of 2D materials. Furthermore, we hope this review inspires future multiscale, theoretical efforts focused on addressing the nontrivial mechanics ingredients (such as elasto-capillarity, long-range vdW interactions, screening effects, and so on) in the wetting statics and dynamics being observed in 2D material systems. By gaining a comprehensive understanding of these intricate wetting behaviors, a broad range of applications where 2D materials meet liquids may be effectively guided and developed.

DECLARATIONS

Authors' contributions
Contribute to the conception, design, and writing of this review: Yu C, Dai Z

Availability of data and materials
Not applicable.

Conflicts of interest
All authors declared that there are no conflicts of interest.

Ethical approval and consent to participate
Not applicable.

Consent for publication
Not applicable.

REFERENCES

1. Radisavljevic B, Radenovic A, Brivio J, Giacometti V, Kis A. Single-layer MoS$_2$ transistors. *Nat Nanotechnol* 2011;6:147-50. DOI PubMed
2. Koppens FHL, Mueller T, Avouris P, Ferrari AC, Vitiello MS, Polini M. Photodetectors based on graphene, other two-dimensional materials and hybrid systems. *Nat Nanotechnol* 2014;9:780-93. DOI PubMed
3. Papageorgiou DG, Kinloch IA, Young RJ. Mechanical properties of graphene and graphene-based nanocomposites. *Prog Mater Sci* 2017;90:75-127. DOI
4. Liu X, Ma T, Pinna N, Zhang J. Two-dimensional nanostructured materials for gas sensing. *Adv Funct Mater* 2017;27:1702168. DOI
5. Khan K, Tareen AK, Aslam M, et al. Recent developments in emerging two-dimensional materials and their applications. *J Mater Chem C* 2020;8:387-440. DOI
6. Yin J, Li X, Yu J, Zhang Z, Zhou J, Guo W. Generating electricity by moving a droplet of ionic liquid along graphene. *Nat Nanotechnol* 2014;9:378-83. DOI PubMed
7. Liu X, Hersam MC. Interface characterization and control of 2D Materials and heterostructures. *Adv Mater* 2018;30:e1801586. DOI
8. Dai Z, Lu N, Liechti KM, Huang R. Mechanics at the interfaces of 2D materials: challenges and opportunities. *Curr Opin Solid State Mater Sci* 2020;24:100837. DOI
9. Aria AI, Kidambi PR, Weatherup RS, Xiao L, Williams JA, Hofmann S. Time evolution of the wettability of supported graphene

under ambient air exposure. *J Phys Chem C Nanomater Interfaces* 2016;120:2215-24. DOI PubMed PMC

10.   Bera B, Shahidzadeh N, Mishra H, Belyaeva LA, Schneider GF, Bonn D. Wetting of water on graphene nanopowders of different thicknesses. *Appl Phys Lett* 2018;112:151606. DOI

11.   Du F, Huang J, Duan H, Xiong C, Wang J. Wetting transparency of supported graphene is regulated by polarities of liquids and substrates. *Appl Surf Sci* 2018;454:249-55. DOI

12.   Kim D, Kim E, Park S, et al. Wettability of graphene and interfacial water structure. *Chem* 2021;7:1602-14. DOI

13.   Kim E, Kim D, Kwak K, Nagata Y, Bonn M, Cho M. Wettability of graphene, water contact angle, and interfacial water structure. *Chem* 2022;8:1187-200. DOI

14.   Ondarçuhu T, Thomas V, Nuñez M, et al. Wettability of partially suspended graphene. *Sci Rep* 2016;6:24237. DOI PubMed PMC

15.   Zhang J, Jia K, Huang Y, et al. Intrinsic wettability in pristine graphene (Adv. Mater. 6/2022). *Adv Mater* 2022;34:e2103620. DOI

16.   Zhao Y, Wang G, Huang W, et al. Investigations on the wettability of graphene on a micron-scale hole array substrate. *RSC Adv* 2016;6:1999-2003. DOI

17.   Chen L, Shi G, Shen J, et al. Ion sieving in graphene oxide membranes via cationic control of interlayer spacing. *Nature* 2017;550:380-3. DOI

18.   Hu S, Lozada-Hidalgo M, Wang FC, et al. Proton transport through one-atom-thick crystals. *Nature* 2014;516:227-30. DOI PubMed

19.   Lozada-Hidalgo M, Hu S, Marshall O, et al. Sieving hydrogen isotopes through two-dimensional crystals. *Science* 2016;351:68-70. DOI PubMed

20.   Joshi RK, Carbone P, Wang FC, et al. Precise and ultrafast molecular sieving through graphene oxide membranes. *Science* 2014;343:752-4. DOI PubMed

21.   Abdolhosseinzadeh S, Zhang C(J), Schneider R, Shakoorioskooie M, Nüesch F, Heier J. A universal approach for room-temperature printing and coating of 2D materials (Adv. Mater. 4/2022). *Adv Mater* 2022;34:2270033. DOI

22.   Wang J, Gao W, Zhang H, Zou M, Chen Y, Zhao Y. Programmable wettability on photocontrolled graphene film. *Sci Adv* 2018;4:eaat7392. DOI PubMed PMC

23.   Das S, Pandey D, Thomas J, Roy T. 2D materials: the role of graphene and other 2D materials in solar photovoltaics (Adv. Mater. 1/2019). *Adv Mater* 2019;31:1970006. DOI

24.   Aryal UK, Ahmadpour M, Turkovic V, Rubahn HG, Di Carlo A, Madsen M. 2D materials for organic and perovskite photovoltaics. *Nano Energy* 2022;94:106833. DOI

25.   Zhou KG, Vasu KS, Cherian CT, et al. Electrically controlled water permeation through graphene oxide membranes. *Nature* 2018;559:236-40. DOI PubMed

26.   Zhu Y, Murali S, Stoller MD, et al. Carbon-based supercapacitors produced by activation of graphene. *Science* 2011;332:1537-41. DOI PubMed

27.   Liu Z, Liu C, Chen Z, et al. Recent advances in two-dimensional materials for hydrovoltaic energy technology. *Exploration* 2023;3:20220061. DOI PubMed PMC

28.   Shih CJ, Wang QH, Lin S, et al. Erratum: breakdown in the wetting transparency of graphene [Phys. Rev. Lett. **109**, 176101 (2012)]. *Phys Rev Lett* 2012;115:049901. DOI

29.   Parobek D, Liu H. Wettability of graphene. *2D Mater* 2015;2:032001. DOI

30.   Leenaerts O, Partoens B, Peeters FM. Water on graphene: hydrophobicity and dipole moment using density functional theory. *Phys Rev B* 2009;79:235440. DOI

31.   Rafiee J, Mi X, Gullapalli H, et al. Wetting transparency of graphene. *Nat Mater* 2012;11:217-22. DOI

32.   Raj R, Maroo SC, Wang EN. Wettability of graphene. *Nano Lett* 2013;13:1509-15. DOI PubMed

33.   Shih CJ, Strano MS, Blankschtein D. Wetting translucency of graphene. *Nat Mater* 2013;12:866-9. DOI PubMed

34.   Zhao G, Li X, Huang M, et al. The physics and chemistry of graphene-on-surfaces. *Chem Soc Rev* 2017;46:4417-49. DOI PubMed

35.   Snapp P, Kim JM, Cho C, Leem J, Haque MF, Nam S. Interaction of 2D materials with liquids: wettability, electrochemical properties, friction, and emerging directions. *NPG Asia Mater* 2020;12:22. DOI

36.   Belyaeva LA, Schneider GF. Wettability of graphene. *Surf Sci Rep* 2020;75:100482. DOI

37.   Xia K, Jian M, Zhang W, Zhang Y. Visualization of graphene on various substrates based on water wetting behavior. *Adv Mater Interfaces* 2016;3:1500674. DOI

38.   Zhao J, Zhu J, Cao R, et al. Liquefaction of water on the surface of anisotropic two-dimensional atomic layered black phosphorus. *Nat Commun* 2019;10:4062. DOI PubMed PMC

39.   Schulman RD, Ledesma-Alonso R, Salez T, Raphaël E, Dalnoki-Veress K. Liquid droplets act as "compass needles" for the stresses in a deformable membrane. *Phys Rev Lett* 2017;118:198002. DOI PubMed

40.   Sanchez DA, Dai Z, Lu N. 2D material bubbles: fabrication, characterization, and applications. *Trends Chem* 2021;3:204-17. DOI

41.   Rao Y, Qiao S, Dai Z, Lu N. Elastic wetting: Substrate-supported droplets confined by soft elastic membranes. *J Mech Phys Solids* 2021;151:104399. DOI

42.   Rao Y, Kim E, Dai Z, He J, Li Y, Lu N. Size-dependent shape characteristics of 2D crystal blisters. *J Mech Phys Solids* 2023;175:105286. DOI

43.   Dai Z, Rao Y, Lu N. Two-dimensional crystals on adhesive substrates subjected to uniform transverse pressure. *Int J Solids Struct* 2022;257:111829. DOI

44.   Ma J, Kim JM, Hoque MJ, et al. Role of thin film adhesion on capillary peeling. *Nano Lett* 2021;21:9983-9. DOI PubMed

45.　Liu H, Thi QH, Man P, et al. Controlled adhesion of ice-toward ultraclean 2D materials (Adv. Mater. 14/2023). *Adv Mater* 2023;35:2370102. DOI

46.　Cai J, Chen H, Ke Y, Deng S. A capillary-force-assisted transfer for monolayer transition-metal-dichalcogenide crystals with high utilization. *ACS Nano* 2022;16:15016-25. DOI PubMed

47.　Zhang Y, Yin M, Baek Y, et al. Capillary transfer of soft films. *Proc Natl Acad Sci U S A* 2020;117:5210-6. DOI PubMed PMC

48.　Gurarslan A, Yu Y, Su L, et al. Surface-energy-assisted perfect transfer of centimeter-scale monolayer and few-layer MoS$_2$ films onto arbitrary substrates. *ACS Nano* 2014;8:11522-8. DOI PubMed

49.　Zhao H, Wang B, Liu F, et al. Fluidic flow assisted deterministic folding of van der Waals materials. *Adv Funct Mater* 2020;30:1908691. DOI

50.　Ferrari GA, de Oliveira AB, Silvestre I, et al. Apparent softening of wet graphene membranes on a microfluidic platform. *ACS Nano* 2018;12:4312-20. DOI PubMed

51.　Chen E, Dai Z. Axisymmetric peeling of thin elastic films: a perturbation solution. *J Appl Mech* 2023;90:101011. DOI

52.　Cao P, Bai P, Omrani AA, et al. Preventing thin film dewetting via graphene capping. *Adv Mater* 2017;29:1701536. DOI

53.　Ares P, Cea T, Holwill M, et al. Piezoelectric materials: piezoelectricity in monolayer hexagonal boron nitride (Adv. Mater. 1/2020). *Adv Mater* 2020;32:e1905504. DOI

54.　Ares P, Wang YB, Woods CR, et al. Van der Waals interaction affects wrinkle formation in two-dimensional materials. *Proc Natl Acad Sci U S A* 2021:118-e2025870118. DOI PubMed PMC

55.　Dai Z, Vella D. Droplets on lubricated surfaces: the slow dynamics of skirt formation. *Phys Rev Fluids* 2022;7:054003. DOI

56.　Hou Y, Dai Z, Zhang S, et al. Elastocapillary cleaning of twisted bilayer graphene interfaces. *Nat Commun* 2021;12:5069. DOI PubMed PMC

57.　Ross FM. Opportunities and challenges in liquid cell electron microscopy. *Science* 2015;350:aaa9886. DOI PubMed

58.　Ghodsi SM, Megaridis CM, Shahbazian-yassar R, Shokuhfar T. Advances in graphene-based liquid cell electron microscopy: working principles, opportunities, and challenges. *Small Methods* 2019;3:1900026. DOI

59.　Zhang J, Lin L, Sun L, et al. Clean transfer of large graphene single crystals for high-intactness suspended membranes and liquid cells. *Adv Mater* 2017;29:1700639. DOI PubMed

60.　Yuk JM, Park J, Ercius P, et al. High-resolution EM of colloidal nanocrystal growth using graphene liquid cells. *Science* 2012;336:61-4. DOI PubMed

61.　Park J, Koo K, Noh N, et al. Graphene liquid cell electron microscopy: progress, applications, and perspectives. *ACS Nano* 2021;15:288-308. DOI PubMed

62.　Park JB, Shin D, Kang S, Cho SP, Hong BH. Distortion in two-dimensional shapes of merging nanobubbles: evidence for anisotropic gas flow mechanism. *Langmuir* 2016;32:11303-8. DOI PubMed

63.　Shin D, Park JB, Kim YJ, et al. Growth dynamics and gas transport mechanism of nanobubbles in graphene liquid cells. *Nat Commun* 2015;6:6068. DOI

64.　Yoshida H, Kaiser V, Rotenberg B, Bocquet L. Dripplons as localized and superfast ripples of water confined between graphene sheets. *Nat Commun* 2018;9:1496. DOI PubMed PMC

65.　Sun JS, Jiang JW, Park HS, Zhang S. Self-cleaning by harnessing wrinkles in two-dimensional layered crystals. *Nanoscale* 2017;10:312-8. DOI PubMed

66.　Sanchez DA, Dai Z, Wang P, et al. Mechanics of spontaneously formed nanoblisters trapped by transferred 2D crystals. *Proc Natl Acad Sci U S A* 2018;115:7884-9. DOI PubMed PMC

67.　Algara-Siller G, Lehtinen O, Wang FC, et al. Square ice in graphene nanocapillaries. *Nature* 2015;519:443-5. DOI

68.　Novoselov KS, Mishchenko A, Carvalho A, Castro Neto AH. 2D materials and van der Waals heterostructures. *Science* 2016;353:aac9439. DOI

69.　Wang S, Zhang Y, Abidi N, Cabrales L. Wettability and surface free energy of graphene films. *Langmuir* 2009;25:11078-81. DOI PubMed

70.　Prydatko AV, Belyaeva LA, Jiang L, Lima LMC, Schneider GF. Contact angle measurement of free-standing square-millimeter single-layer graphene. *Nat Commun* 2018;9:4185. DOI PubMed PMC

71.　Wang H, Orejon D, Song D, et al. Non-wetting of condensation-induced droplets on smooth monolayer suspended graphene with contact angle approaching 180 degrees. *Commun Mater* 2022;3:75. DOI

72.　Bico J, Reyssat É, Roman B. Elastocapillarity: when surface tension deforms elastic solids. *Annu Rev Fluid Mech* 2018;50:629-59. DOI

73.　Lin L, Zhang J, Su H, et al. Towards super-clean graphene. *Nat Commun* 2019;10:1912. DOI PubMed PMC

74.　Choi J, Mun J, Wang MC, Ashraf A, Kang SW, Nam SW. Hierarchical, dual-scale structures of atomically thin MoS$_2$ for tunable wetting. *Nano Lett* 2017;17:1756-61. DOI PubMed

75.　Gaire B, Singla S, Dhinojwala A. Screening of hydrogen bonding interactions by a single layer graphene†. *Nanoscale* 2021;13:8098-106. DOI PubMed

76.　Li Z, Wang Y, Kozbial A, et al. Effect of airborne contaminants on the wettability of supported graphene and graphite. *Nat Mater* 2013;12:925-31. DOI PubMed

77.　Kim GT, Gim SJ, Cho SM, Koratkar N, Oh IK. Wetting-transparent graphene films for hydrophobic water-harvesting surfaces. *Adv Mater* 2014;26:5166-72. DOI PubMed

78. Shin YJ, Wang Y, Huang H, et al. Surface-energy engineering of graphene. *Langmuir* 2010;26:3798-802. DOI

79. Lai CY, Tang TC, Amadei CA, et al. A nanoscopic approach to studying evolution in graphene wettability. *Carbon* 2014;80:784-92. DOI

80. Kozbial A, Li Z, Sun J, et al. Understanding the intrinsic water wettability of graphite. *Carbon* 2014;74:218-25. DOI

81. Gurarslan A, Jiao S, Li TD, et al. Van der Waals force isolation of monolayer MoS_2. *Adv Mater* 2016;28:10055-60. DOI PubMed

82. Chow PK, Singh E, Viana BC, et al. Wetting of mono and few-layered WS_2 and MoS_2 films supported on Si/SiO_2 substrates. *ACS Nano* 2015;9:3023-31. DOI PubMed

83. Singh B, Ali N, Chakravorty A, Sulania I, Ghosh S, Kabiraj D. Wetting behavior of MoS_2 thin films. *Mater Res Express* 2019;6:096424. DOI

84. Li S, Liu K, Klimeš J, Chen J. Understanding the wetting of transition metal dichalcogenides from an *ab initio* perspective. *Phys Rev Res* 2023;5:023018. DOI

85. Rodrigues SP, Evaristo M, Carvalho S, Cavaleiro A. Fluorine-carbon doping of WS-based coatings deposited by reactive magnetron sputtering for low friction purposes. *Appl Surf Sci* 2018;445:575-85. DOI

86. Liu X, Zhang Z, Guo W. van der Waals screening by graphenelike monolayers. *Phys Rev B* 2018;97:241411. DOI

87. Wagemann E, Wang Y, Das S, Mitra SK. On the wetting translucency of hexagonal boron nitride†. *Phys Chem Chem Phys* 2020;22:7710-8. DOI PubMed

88. Wagemann E, Wang Y, Das S, Mitra SK. Wettability of nanostructured hexagonal boron nitride surfaces: molecular dynamics insights on the effect of wetting anisotropy. *Phys Chem Chem Phys* 2020;22:2488-97. DOI PubMed

89. Li X, Qiu H, Liu X, Yin J, Guo W. Wettability of supported monolayer hexagonal boron nitride in air. *Adv Funct Mater* 2017;27:1603181. DOI

90. Chen X, Yang Z, Feng S, et al. How universal is the wetting aging in 2D materials. *Nano Lett* 2020;20:5670-7. DOI PubMed

91. Wang FC, Wu HA. Pinning and depinning mechanism of the contact line during evaporation of nano-droplets sessile on textured surfaces. *Soft Matter* 2013;9:5703-9. DOI

92. Wang L, Lu N. Conformability of a thin elastic membrane laminated on a soft substrate with slightly wavy surface. *J Appl Mech* 2016;83:041007. DOI

93. Gao W, Huang R. Effect of surface roughness on adhesion of graphene membranes. *J Phys D Appl Phys* 2011;44:452001. DOI

94. Wagner TJW, Vella D. The sensitivity of graphene "snap-through" to substrate geometry. *Appl Phys Lett* 2012;100:233111. DOI

95. Liu S, He J, Rao Y, et al. Conformability of flexible sheets on spherical surfaces. *Sci Adv* 2023;9:eadf2709. DOI PubMed PMC

96. Box F, Domino L, Corvo TO, et al. Delamination from an adhesive sphere: Curvature-induced dewetting versus buckling. *Proc Natl Acad Sci U S A* 2023;120:e2212290120. DOI PubMed PMC

97. Du F, Huang J, Duan H, Xiong C, Wang J. Surface stress of graphene layers supported on soft substrate. *Sci Rep* 2016;6:25653. DOI PubMed PMC

98. Fang Z, Dai Z, Wang B, et al. Pull-to-peel of two-dimensional materials for the simultaneous determination of elasticity and adhesion. *Nano Lett* 2023;23:742-9. DOI

99. Dai Z, Hou Y, Sanchez DA, et al. Interface-governed deformation of nanobubbles and nanotents formed by two-dimensional materials. *Phys Rev Lett* 2018;121:266101. DOI

100. Dai Z, Liu L, Zhang Z. 2D materials: strain engineering of 2D materials: issues and opportunities at the interface (Adv. Mater. 45/2019). *Adv Mater* 2019;31:1970322. DOI

101. Dai Z, Lu N. Poking and bulging of suspended thin sheets: slippage, instabilities, and metrology. *J Mech Phys Solids* 2021;149:104320. DOI

102. Dai Z, Sanchez DA, Brennan CJ, Lu N. Radial buckle delamination around 2D material tents. *J Mech Phys Solids* 2020;137:103843. DOI

103. Deng S, Berry V. Wrinkled, rippled and crumpled graphene: an overview of formation mechanism, electronic properties, and applications. *Mater Today* 2016;19:197-212. DOI

104. Zang J, Ryu S, Pugno N, et al. Multifunctionality and control of the crumpling and unfolding of large-area graphene. *Nat Mater* 2013;12:321-5. DOI PubMed PMC

105. Ashraf A, Wu Y, Wang MC, et al. Doping-induced tunable wettability and adhesion of graphene. *Nano Lett* 2016;16:4708-12. DOI PubMed

106. Hong G, Han Y, Schutzius TM, et al. On the mechanism of hydrophilicity of graphene. *Nano Lett* 2016;16:4447-53. DOI PubMed

107. van Engers CD, Cousens NEA, Babenko V, et al. Direct measurement of the surface energy of graphene. *Nano Lett* 2017;17:3815-21. DOI PubMed

108. Johnson KL, Greenwood JA. An adhesion map for the contact of elastic spheres. *J Colloid Interf Sci* 1997;192:326-33. DOI PubMed

109. Tiwari A, Wang J, Persson BNJ. Adhesion paradox: why adhesion is usually not observed for macroscopic solids. *Phys Rev E* 2020;102:042803. DOI

110. Tsoi S, Dev P, Friedman AL, et al. van der Waals screening by single-layer graphene and molybdenum disulfide. *ACS Nano* 2014;8:12410-7. DOI PubMed

111. Suk JW, Na SR, Stromberg RJ, et al. Probing the adhesion interactions of graphene on silicon oxide by nanoindentation. *Carbon* 2016;103:63-72. DOI

112.   Li B, Yin J, Liu X, et al. Probing van der Waals interactions at two-dimensional heterointerfaces. *Nat Nanotechnol* 2019;14:567-72. DOI

113.   Lambert AG, Davies PB, Neivandt DJ. Implementing the theory of sum frequency generation vibrational spectroscopy: a tutorial review. *Appl Spectrosc Rev* 2005;40:103-45. DOI

114.   Morita A, Ishiyama T. Recent progress in theoretical analysis of vibrational sum frequency generation spectroscopy. *Phys Chem Chem Phys* 2008;10:5801-16. DOI PubMed

115.   Nagata Y, Mukamel S. Vibrational sum-frequency generation spectroscopy at the water/lipid interface: molecular dynamics simulation study. *J Am Chem Soc* 2010;132:6434-42. DOI PubMed PMC

116.   Singla S, Anim-Danso E, Islam AE, et al. Insight on structure of water and ice next to graphene using surface-sensitive spectroscopy. *ACS Nano* 2017;11:4899-906. DOI PubMed

117.   Dreier LB, Liu Z, Narita A, et al. Surface-specific spectroscopy of water at a potentiostatically controlled supported graphene monolayer. *J Phys Chem C* 2019;123:24031-8. DOI PubMed PMC

118.   Castro FJ, Meyer G. Thermal desorption spectroscopy (TDS) method for hydrogen desorption characterization (I): theoretical aspects. *J Alloys Compd* 2002;330-2:59-63. DOI

119.   von Zeppelin F, Haluška M, Hirscher M. Thermal desorption spectroscopy as a quantitative tool to determine the hydrogen content in solids. *Thermochim Acta* 2003;404:251-8. DOI

120.   Belyaeva LA, Tang C, Juurlink L, Schneider GF. Macroscopic and microscopic wettability of graphene. *Langmuir* 2021;37:4049-55. DOI PubMed PMC